

F



\*X1999-00478\*

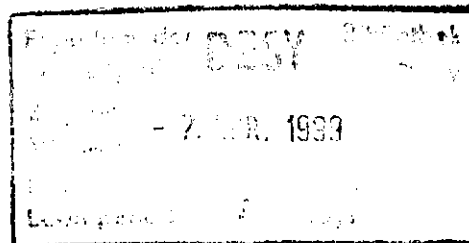
Internal Report  
DESY D3-94  
March 1999

# The Field of Scattered Radiation in the Tunnel of the Proton Storage Ring HERA Measurements and Calculations

H. Dinter, A. Leuschner, K. Tesch  
Deutsches Elektronen-Synchrotron DESY, Hamburg, Germany

and

D. Dworak  
Institute of Nuclear Physics, Krakow, Poland



**DESY behält sich alle Rechte für den Fall der Schutzrechtserteilung und für die wirtschaftliche Verwertung der in diesem Bericht enthaltenen Informationen vor.**

**DESY reserves all rights for commercial use of information included in this report, especially in case of filing application for or grant of patents.**

**"Die Verantwortung für den Inhalt dieses  
Internen Berichtes liegt ausschließlich beim Verfasser"**

Internal Report  
DESY D3-94  
March 1999

# **The Field of Scattered Radiation in the Tunnel of the Proton Storage Ring HERA Measurements and Calculations**

H. Dinter, A. Leuschner, K. Tesch  
Deutsches Elektronen-Synchrotron DESY, Hamburg, Germany

and

D. Dworak  
Institute of Nuclear Physics, Krakow, Poland

## **Abstract:**

The field of scattered radiation produced by a stored 820-GeV proton beam in the HERA tunnel is studied. Some radiation components are measured by means of conventional instruments, the results are compared with calculations using the FLUKA Monte Carlo code. Good absolute agreement is received. This agreement justifies the calculation of spectra, integrated fluences and integrated doses of scattered neutrons, protons, pions, electrons, positrons, and photons which are produced by interaction of the primary beam with a collimator or with the rest gas in a drastically simplified geometry of the long accelerator structure.



## 1. Introduction

The field of scattered radiation produced by a high energy proton beam and penetrating the accelerator shielding is well known both by measurements and by calculations, recent papers are given in [1] – [6]. Not many systematic studies are available on the radiation field, i.e. the spectra of produced secondary particles, inside the accelerator room. Such a field is produced by the beam halo hitting the vacuum chamber or a collimator or by the interaction of the proton beam with the rest gas. This subject is not covered by the numerous measurements and calculations of secondary particle spectra produced around thick targets. The first measurements in an accelerator room were performed at the FNAL, the spectra of low energy neutrons in the Tevatron tunnel produced by interaction with the rest gas were studied [7]. Such a neutron field inside the Tevatron tunnel or inside the HERA tunnel at DESY was calculated in [8] – [10]. Other internal reports give calculations of neutron and charged hadron fields above 500 MeV [11] and also at lower energies [12].

A knowledge of the field of scattered radiation inside the tunnel is of importance for several reasons:

- (a) it gives information on necessary shieldings and for understanding the radiation field outside the shield,
- (b) it can be useful for estimation of the background of measuring devices in the tunnel or possible radiation damages,
- (c) experimental data check the usefulness of applying Monte Carlo codes with simplified tunnel geometries,
- (d) it can give rough criteria to estimate doses if a person is left back in the tunnel during operation in case of an accident.

Therefore a new approach was started in 1996 to study scattered radiations in the tunnel of the storage ring HERA with an 820-GeV proton beam. The experimental possibilities of measuring particle spectra below 1 GeV in such an environment are rather limited. We used simple instruments usually in use outside shieldings to measure particle fluences and doses. It is not obvious that they can be used also in an accelerator room. The interpretation of their readings need the confirmation by accompanying calculations. For such calculations the FLUKA Monte Carlo code [13] is very suitable. Its high energy part was checked in many experiments. The low energy part important for the problems under study was improved in the last years. The greatest uncertainties arise from the limited approach to model the details of a 100 m long tunnel section for the Monte Carlo process. The measurements and calculations described in the present paper enable us to make several comparisons between both. Not only relative comparisons but in some cases also absolute comparisons are possible to see if experiments and calculations support each other.

The locations in the HERA tunnel and examined modes of accelerator operation are described in section 2. The greatly simplified geometries suitable for Monte Carlo calculations are sketched. They refer to two standard cases: the interaction between the beam halo and a collimator and the beam rest gas interaction. The used instruments are described in section 3. Section 4 contains the comparison between measurements and calculations for some special cases. In section 5 the calculated spectra of produced neutrons, protons, positive and negative pions, positrons, electrons and photons in the full energy range below 1 GeV are presented. Integrated fluences and doses are also given.

## 2. Tunnel Geometries and Modes of Accelerator Operation

The experiments were performed in a long straight section of the HERA proton storage ring (comprising Hall West) in three different geometries and modes of accelerator operation. In geometry Ia the instruments were placed 130 m downstream of a tungsten collimator and at a radial distance of 60 – 140 cm to the vacuum pipe, so they were "looking" against the pro-

ton beam at small angles. The collimator is moved near to the beam in normal storage ring operation to minimize the background at the high energy experiment located in the next hall downstream. Between the collimator and our instruments 8 quadrupole magnets, 3 sextupole magnets, and 8 kicker magnets (belonging to the beam abort system) were positioned along the beam line. This arrangement is drastically simplified for the calculations and is shown in fig. 1. A cylindrical geometry was adopted with a 2.5 cm thick iron beam pipe which simulates the material near to the beam, and the beam halo is simulated by a hollow beam with inner radius 1.0 cm and outer radius 1.5 cm, hitting a collimator with inner radius 1.0 cm and outer radius 3 cm. Seven plane ring-shaped "detectors" are placed downstream of the collimator, their radial distance to the beam is 50 – 130 cm. The number of protons intercepted by the collimator during the measurements could not be measured, therefore only relative comparisons between calculations and measurements are possible, see section 4.

In cases the collimator was opened totally, the production of secondary particles was due only to the interaction with the rest gas of the straight section. The gas pressure was  $6 \cdot 10^{-9}$  mbar on the average with an uncertainty of a factor of 2 in both directions. The stored beam current was measured, and the electronic instruments were gated to measure only this case which we call geometry Ib. It is simulated with a geometry as in fig. 1 but with the collimator removed and with a one-dimensional beam interacting with the rest gas in the vacuum chamber. The assumed rest gas consists of 90% H<sub>2</sub> and 10% N<sub>2</sub> (according to measurements) at a pressure of 1000 mbar; the calculated results are linearly scaled down to  $6 \cdot 10^{-9}$  mbar which is justified since at 1000 mbar the total and inelastic interaction lengths of protons in nitrogen are 420 m and 700 m, respectively. This geometry offers a comparison on an absolute base between measurements and calculations.

The scattered radiation was not only studied at small angles but also at angles around 90° to the beam (geometry II). The measurements were performed in Hall West where a high energy experiment was under construction. The radial distance of the measuring devices to the beam was 3.5 m whereas the tunnel radius is 2.5 m. This location and also some massive iron shielded against secondaries produced at small angles. The observed beam pipe was free of magnets or kickers in this case. The geometry II simplified for Monte Carlo calculations is cylindrically symmetric and is shown in fig. 2. Again a one-dimensional beam enters the rest gas in the vacuum chamber. The composition of heavy concrete used as a shield is 58% Fe, 35% O, 4% Ca, 2% Si, 0.6% H, density = 3.7 g/cm<sup>3</sup>.

HERA is an electron-proton collider. The measurements in geometry Ib were made without the electron beam. We found that for geometry Ia and II the background from the electron beam was small compared with other systematic uncertainties.

### 3. The Instruments

The following properties of the scattered radiation field were measured by means of conventional instruments:

- neutron spectra between 1 keV and 1 GeV,
- integrated neutron dose equivalents,
- fluences of charged particles.

They allow a check of consistency between measurements and calculations.

Neutron spectra were measured by passive detectors, a set of polyethylene spheres (diameters 5.1 – 45 cm) with pairs of <sup>6</sup>LiF/ <sup>7</sup>LiF thermoluminescence dosimeters in their centres. The energy range was extended by fission track detectors, thorium or bismuth sheets in contact with polycarbonate foils. The instruments and the procedure to unfold the spectrum are described in [14]. From the fluence spectrum the dose equivalent is calculated by means of conversion factors, we apply the same factors as in [4b]. Three active neutron dosimeters

were used, the commercial Anderson-Braun "rem-meter" (AB in the following) for measuring neutron doses from thermal energy to 20 MeV; the "Linus" (L), a dosimeter with extended energy range up to 300 MeV [3], and a special dosimeter for high energy neutrons above 20 MeV (DHN). The latter is a specially calibrated plastic scintillation counter [15].

They all are calibrated by low energy neutron sources or in neutron fields behind shielding of an accelerator. It is *a priori* not clear if the use of these calibration constants is justified in an accelerator room. In addition, they all are sensitive to high energy protons, pions, electrons and photons. Therefore the experimental results need support from accompanying calculations in the same way as the calculations need the agreement with measurements. The consistency of measurements and calculations is pointed out in section 4.

A simple coincidence unit measured the current of all charged particles: two scintillation counters with  $4 \times 4 \times 0.3 \text{ cm}^3$  NE 110 scintillators. The thresholds of the discriminators were determined by means of commercial  $\gamma$ -sources and in the measuring position during accelerator operation. Counting losses were negligible for all active counters.

#### 4. Measurements and Comparison with Calculations

The variation of the fluences of produced neutrons, protons and pions in beam direction is shown in fig. 3 and 4 for the geometries Ia and Ib. Fig. 3 gives the strong decrease behind a collimator hit by the halo of the proton beam, and in fig. 4 the build-up of the fluences behind the first interaction between beam and rest gas is calculated. We take the point at 50 m as being representative for the radiation field in the tunnel, since at distances larger than 20 m the calculated particle spectra are more or less constant (fig. 3), and an equilibrium is reached (fig. 4); all calculated results given below refer to this point. All results concerning beam-gas interaction are scaled down to the actual pressure of  $6 \cdot 10^{-9}$  mbar.

The radial dependence of the radiation field was measured with a string of  $^7\text{LiF}$  thermoluminescence dosimeters, the results show independence of radial distance between 50 cm and 140 cm. The instruments and also the scoring surfaces of the Monte Carlo calculations were placed at these positions. At a distance of 30 cm, 10 cm, and on the vacuum pipe the measured dose was higher by a factor of 2, 3, and 10, respectively.

First we compare some measured results received with the active neutron dosimeters and with the passive neutron spectrometer (n-spec) mentioned in the preceding section. From the neutron fluence spectrum the total dose equivalent or particle doses above and below 20 MeV are calculated. Dose ratios are entered into the first three lines of tab. 1. Their values are not far away from unity expected in the ideal case though the instruments and their conventional calibration constants are completely different. It proves that they can be used with confidence in the tunnel environment. The other two lines of tab. 1 give measured and calculated neutron dose ratios for the same case (beam halo hitting the collimator), a satisfying agreement is obtained.

The neutron spectra are shown in fig. 5. The calculated spectra are normalized to one incoming 820-GeV proton. The measurements with the passive spectrometer were taken in periods of several weeks, the number of primary protons could not be determined, therefore the results are normalized in a way that the low energy peak has the same height as the calculated peak. Measurements and calculations give qualitative agreement. The spectrum in fig. 5 A has the same shape, as found behind concrete shielding: a contribution of high energy neutrons around 100 MeV from the intranuclear cascade, and the peak of evaporation neutrons around 1 MeV. The high energy neutrons nearly disappear in case of geometry II, as expected.

Measurements		Calculations	
H (L) / H (tot, n spec)	0.91		
H (A B) / H (< 20 MeV, n-spec)	1.3		
H (DHN) / H(> 20 MeV, n-spec)	1.1		
H (L) / H (AB)	1.8	H (tot) / H (< 20 MeV)	2.2
H (DHN) / H (AB)	1.1	H (> 20 MeV) / H (< 20 MeV)	1.2

Tab. 1. Comparison of instruments measuring neutron doses and ratios of neutron doses received by measurements and calculations for geometry Ia.

An absolute comparison, i.e. a comparison between measured and calculated doses per incoming proton, is presented in tab. 2. The ratios of calculated to measured doses scatter around 2. A better agreement cannot be expected since the actual gas pressure enters into this comparison which is known only with an error of a factor of 2.

Geometry	Measurement		Calculation		Calc./Meas.
Ib	H (L)	$1.2 \cdot 10^{-26}$ Sv	H (tot)	$2.5 \cdot 10^{-26}$ Sv	2.1
	H (AB)	$5.0 \cdot 10^{-27}$ Sv	H (< 20 MeV)	$1.6 \cdot 10^{-26}$ Sv	3.2
	H (DHN)	$6.0 \cdot 10^{-27}$ Sv	H (> 20 MeV)	$9.3 \cdot 10^{-27}$ Sv	1.5
II	H (L)	$1.3 \cdot 10^{-26}$ Sv	H (tot)	$1.0 \cdot 10^{-26}$ Sv	0.8
	H (AB)	$1.2 \cdot 10^{-26}$ Sv	H (< 20 MeV)	$9.1 \cdot 10^{-27}$ Sv	0.8

Tab. 2. Measured and calculated neutron dose equivalents per one 820-GeV proton hitting the rest gas at a pressure of  $6 \cdot 10^{-9}$  mbar.

A similar comparison is made between the results of our coincidence unit and the calculated current of scattered protons, pions, electrons, and positrons. A correction was necessary because of the finite distance of the two scintillators and due to the instrumental cut in the particle spectra (see next section) imposed by the detector thresholds. Then the ratios are 1.8 (geometry Ib) and 1.1 (geometry II).

We can state as a main result that measurements and calculations support each other though the instruments are not designed for use in a tunnel environment, and though the tunnel geometry was drastically simplified for the Monte Carlo calculations. The radiation field does not depend on the details of the accelerator structure. Therefore the calculations presented in the next section can be taken as general results for a high energy proton accelerator if the considered geometries are realized.

## 5. Calculation of Scattered Radiation Fields

The spectra of scattered neutrons, protons, and pions per incoming 820-GeV proton hitting either a collimator (geometry Ia) or the rest gas (geometry Ib or II) are displayed in fig. 6. They are averaged over radial distances 50 – 130 cm. The low energy cut is 1 keV for neutrons and 10 MeV for protons and pions. Integrated fluences and doses are given in tab. 3.

Particle	Geometry Ia		Geometry Ib		Geometry II	
	$\Phi$ (cm <sup>-2</sup> )	H (Sv)	$\Phi$ (cm <sup>-2</sup> )	H (Sv)	$\Phi$ (cm <sup>-2</sup> )	H (Sv)
n > 20 MeV	$3.6 \cdot 10^{-6}$	$2.2 \cdot 10^{-15}$	$1.6 \cdot 10^{-17}$	$9.3 \cdot 10^{-27}$	$2.0 \cdot 10^{-18}$	$9.6 \cdot 10^{-28}$
n < 20 MeV	$8.3 \cdot 10^{-6}$	$1.0 \cdot 10^{-15}$	$6.6 \cdot 10^{-17}$	$1.6 \cdot 10^{-26}$	$9.6 \cdot 10^{-17}$	$9.1 \cdot 10^{-27}$
p	$1.1 \cdot 10^{-6}$	$4.6 \cdot 10^{-15}$	$4.3 \cdot 10^{-18}$	$1.8 \cdot 10^{-26}$	$4.3 \cdot 10^{-19}$	$2.3 \cdot 10^{-27}$
$\pi^+$	$7.9 \cdot 10^{-7}$	$1.5 \cdot 10^{-15}$	$5.4 \cdot 10^{-18}$	$9.0 \cdot 10^{-27}$	$2.2 \cdot 10^{-19}$	$3.9 \cdot 10^{-28}$
$\pi^-$	$7.5 \cdot 10^{-7}$	$3.8 \cdot 10^{-15}$	$5.3 \cdot 10^{-18}$	$3.0 \cdot 10^{-26}$	$2.3 \cdot 10^{-19}$	$3.0 \cdot 10^{-27}$

Tab. 3. Integrated hadron fluences  $\Phi$  and dose equivalents H, per incoming 820-GeV proton; gas pressure  $6 \cdot 10^{-9}$  mbar (geometry Ib and II).

The relative contribution of the radiation components is not very different in the geometries I a and I b, whereas in geometry II where particles at small angles to the beam are not detected the fluences of the cascade particles are small and the dose is dominated by low energy neutrons. It is interesting to note that in all cases the negative pions give an important contribution to the total dose due to their high fluence-to-dose conversion factor at energies below 100 MeV.

The production of electrons, positrons, and photons was also studied. They can be produced within the electromagnetic cascade (initiated by  $\pi^0$  decay), by nuclear processes, and by capture of thermal neutrons. The importance of the different mechanisms is seen from tab. 4.

Particle	$\Phi$ (cm <sup>-2</sup> )		
	A	B	C
$e^-$	$3.4 \cdot 10^{-17}$	$3.5 \cdot 10^{-18}$	$3.3 \cdot 10^{-18}$
$e^+$	$1.4 \cdot 10^{-17}$	$1.4 \cdot 10^{-18}$	$1.3 \cdot 10^{-18}$
$\gamma$	$2.1 \cdot 10^{-15}$	$2.2 \cdot 10^{-16}$	$2.0 \cdot 10^{-16}$

Tab. 4. Particle fluences per incoming proton from 3 production modes (see text), geometry Ib.

In case A the full analogue program is used but a cut at 1 keV is applied in the neutron spectrum to prevent neutron capture. In case B the  $\pi^0$  decay is switched off but neutrons are calculated down to thermal energy. Case C also means no  $\pi^0$  decay, a cut of 1 MeV for neutrons is applied. Apparently the electromagnetic cascade (initiated by the  $\pi^0$ -decay) is the main source of the particles, neutron capture is nearly negligible.

The total spectra of electrons, positrons, and photons are displayed in fig. 7, and the integrated fluences and doses are given in tab. 5. The dose due to these particles is nearly as large as the hadron dose. In geometry II electrons and positrons give a large contribution to the total dose (in addition to low energy neutrons), they are scattered into large angles due to multiple Coulomb scattering.

Particle	Geometry Ib		Geometry II	
	$\Phi$ (cm <sup>-2</sup> )	H (Sv)	$\Phi$ (cm <sup>-2</sup> )	H (Sv)
e <sup>-</sup>	3.7·10 <sup>-17</sup>	1.9·10 <sup>-26</sup>	2.4·10 <sup>-17</sup>	1.3·10 <sup>-26</sup>
e <sup>+</sup>	1.5·10 <sup>-17</sup>	6.6·10 <sup>-27</sup>	1.1·10 <sup>-17</sup>	5.6·10 <sup>-27</sup>
$\gamma$	2.3·10 <sup>-15</sup>	1.3·10 <sup>-26</sup>	5.4·10 <sup>-16</sup>	1.6·10 <sup>-27</sup>

Tab. 5. Integrated particle fluences  $\Phi$  and dose equivalents H, per incoming 820-GeV proton, gas pressure  $6 \cdot 10^{-9}$  mbar.

With the given data a total dose rate can be calculated for special cases. An example: An undisturbed proton beam of 100 mA at HERA interacting only with the rest gas ( $6 \cdot 10^{-9}$  mbar) produces rather low dose rates due to all considered particles, 300  $\mu$ Sv/h in the tunnel at a radial distance larger than 50 cm from the beam, and 80  $\mu$ Sv/h in Hall West (distance 3.5 m).

## 6. Literature

1. Landolt-Börnstein, Numerical Data in Science and Technology, N S, vol 11, Springer Verlag (1990)
2. L.E. Moritz, Review of Proton Accelerator Shielding Problems, OECD/NEA Specialists' Meeting, Arlington (1994)
3. C. Birattari, E. DePonti, A. Esposito, A. Ferrari, M. Pellicioni, M. Silari, Nucl. Instr. Meth. A 338 (1994) 534
4. H. Dinter, K. Tesch, D. Dworak, a) Nucl. Instr. Meth. A 368 (1996) 265 and 273, b) Nucl. Instr. Meth. A 384 (1997) 539
5. H. Dinter, K. Tesch, Rad. Prot. Dosimetry 63 (1996) 175
6. I.L. Azhgirey, I.A. Kurochkin, A.V. Sannikov, E.N. Savitskaja, Nucl. Instr. Meth. A 408 (1998) 535
7. J.B. McCaslin, R.S. Sun, W.P. Swanson, J.D. Cossaint, A.J. Elwyn, W.S. Freeman, H. Jöstlein, C.D. Moore, P.M. Yurista, D.E. Groom, Radiation Environment in the Tunnel of a Proton Accelerator near 1 TeV, Congress IRPA, Sydney (1988)
8. R.E. Alsmiller, F.S. Alsmiller, T.A. Gabriel, O.W. Hermann, J.M. Barnes, Nucl. Instr. Meth. A 295 (1990) 99
9. K. Tesch, J.M. Zazula, Report DESY HERA 90-18 (1990)
10. H.J. Möhring, K. Noack, J.M. Zazula, Nucl. Instr. Meth. A 300 (1991) 188
11. R. Brinkmann, Report DESY HERA 87-19 (1987)
12. G.R. Stevenson, J.M. Zazula, Internal Report CERN/TIS-RP/IR/91-20 (1991)
13. A. Fasso, A. Ferrari, P. Sala, FLUKA Code, Version 97 and 98

14. H. Dinter, K. Tesch, Rad. Prot. Dosimetry 42 (1992) 5

15. H. Dinter, B. Racky, K. Tesch, Nucl. Instr. Meth. A 376 (1996) 104

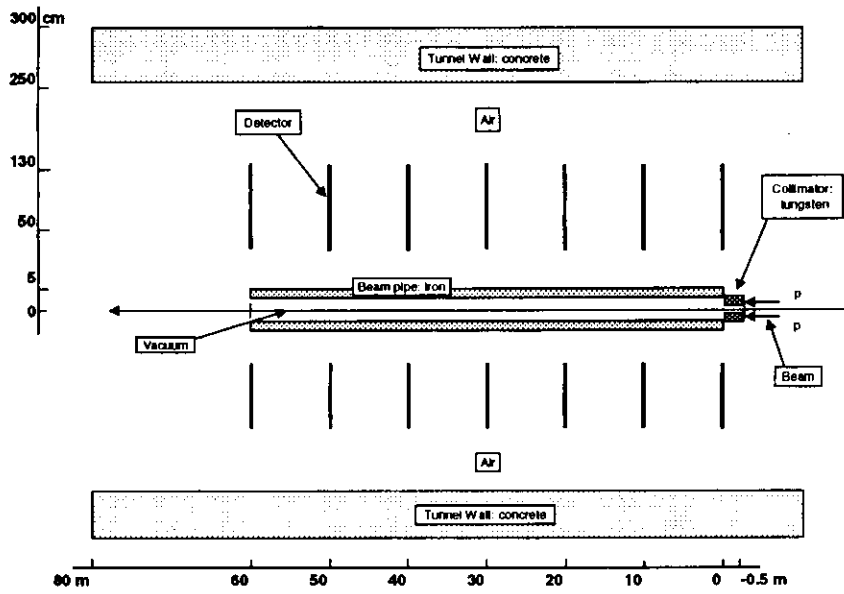


Figure 1: Geometry Ia, simplified for Monte Carlo calculations

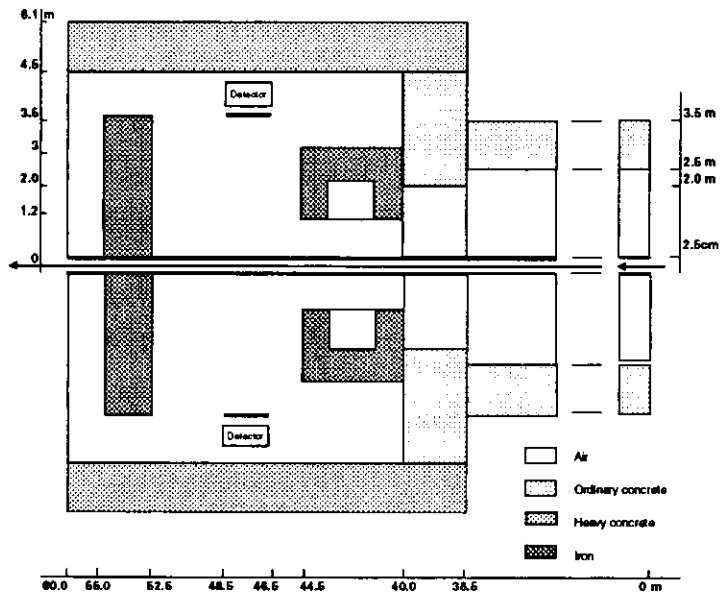


Figure 2: Geometry II, simplified for Monte Carlo Calculations

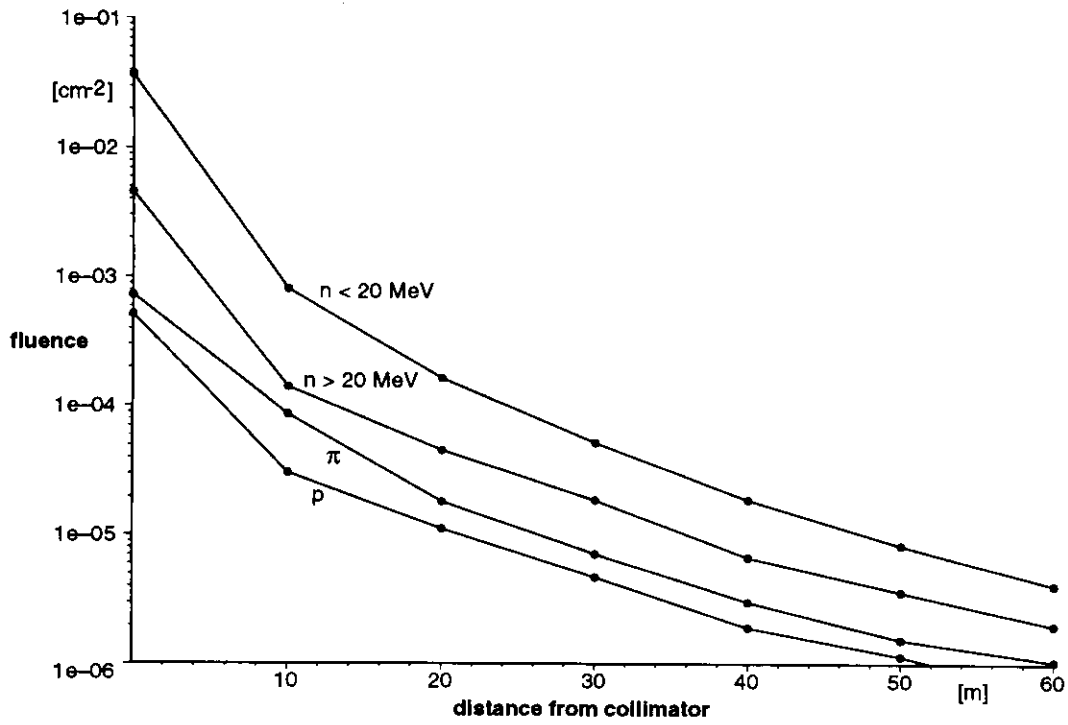


Figure 3: Calculated fluence per primary proton vs. distance from the collimator, geometry Ia.

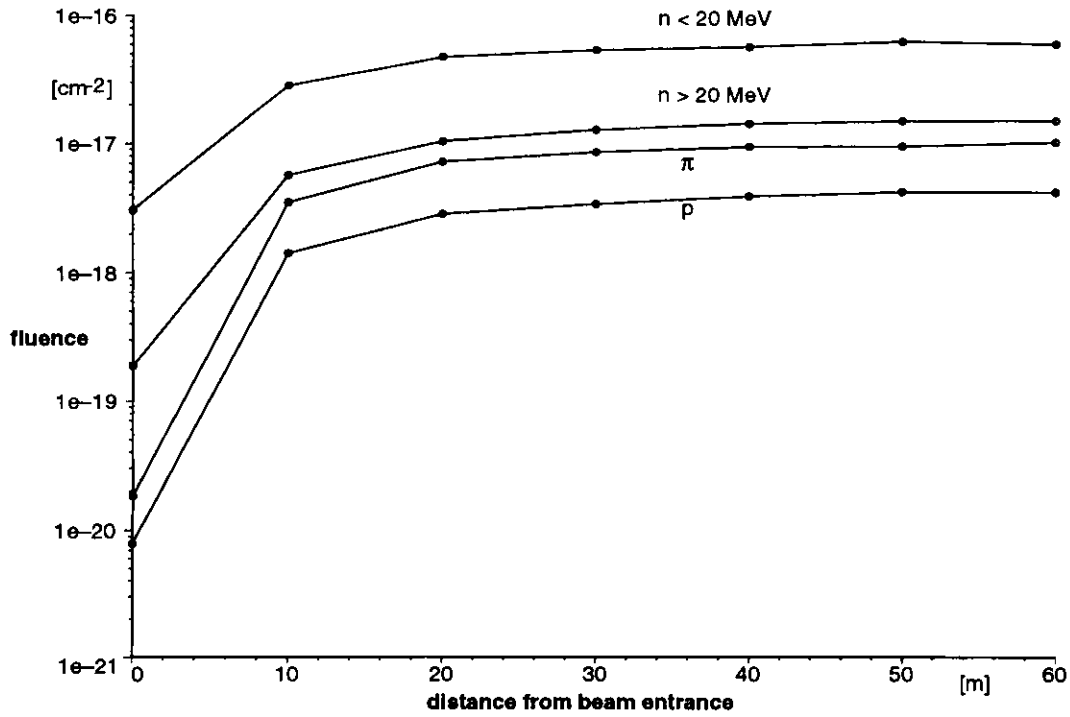


Figure 4: Calculated fluence per primary proton vs. distance from beam entrance, geometry Ib.

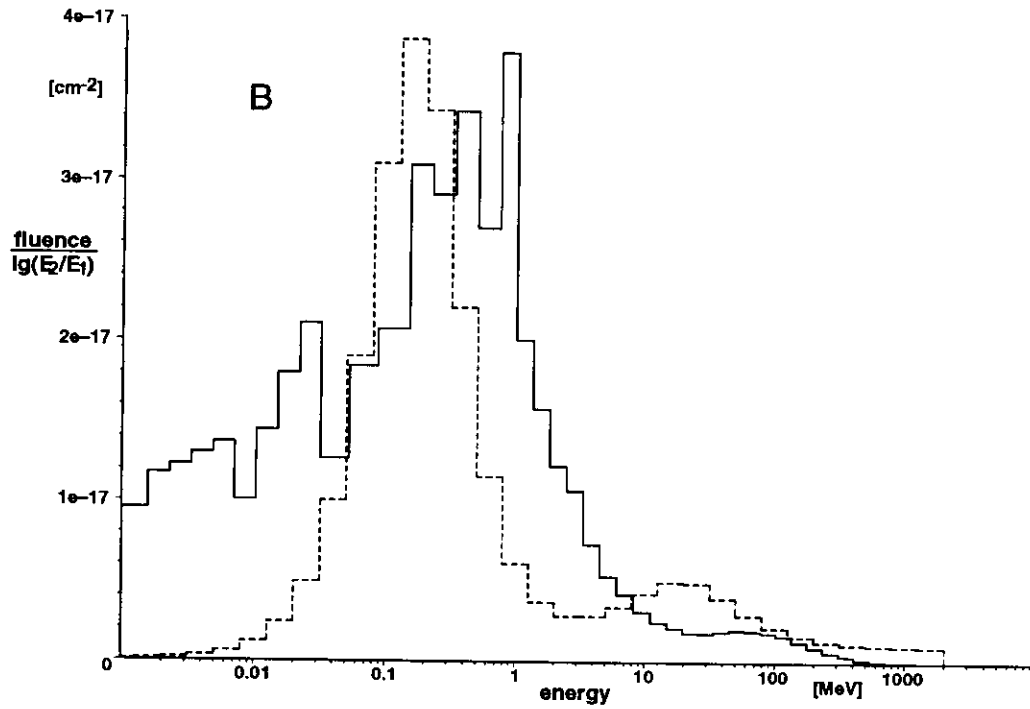
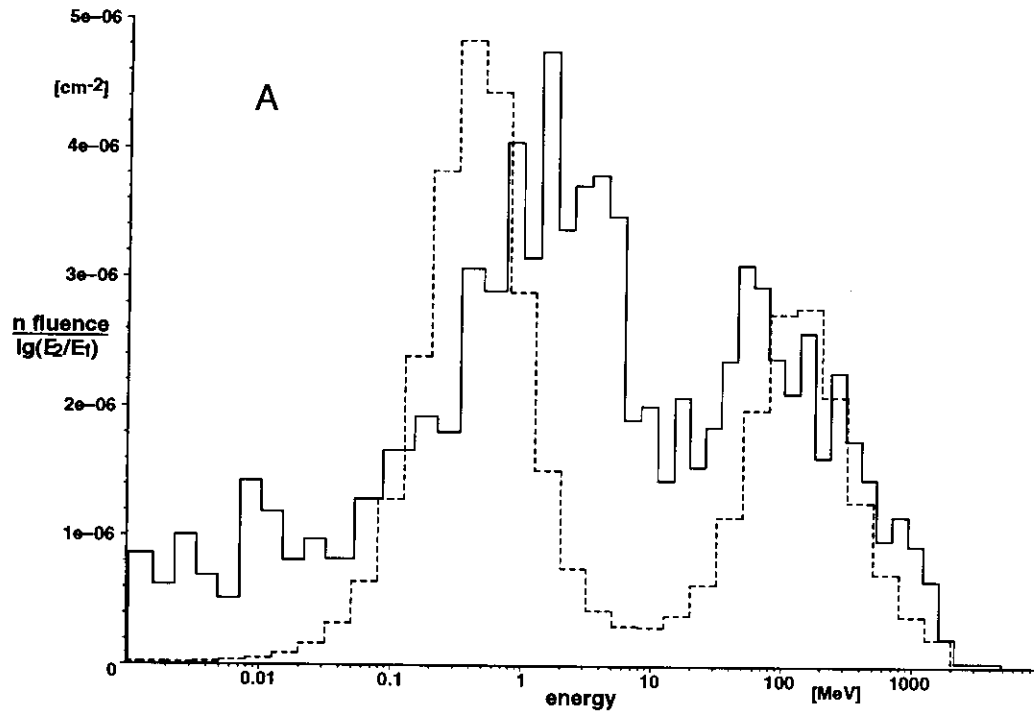


Figure 5: Neutron fluence per logarithmic energy interval per primary proton: FLUKA calculation (solid line), measurements (dashed line, normalized). A) Geometry Ia, B) Geometry II.

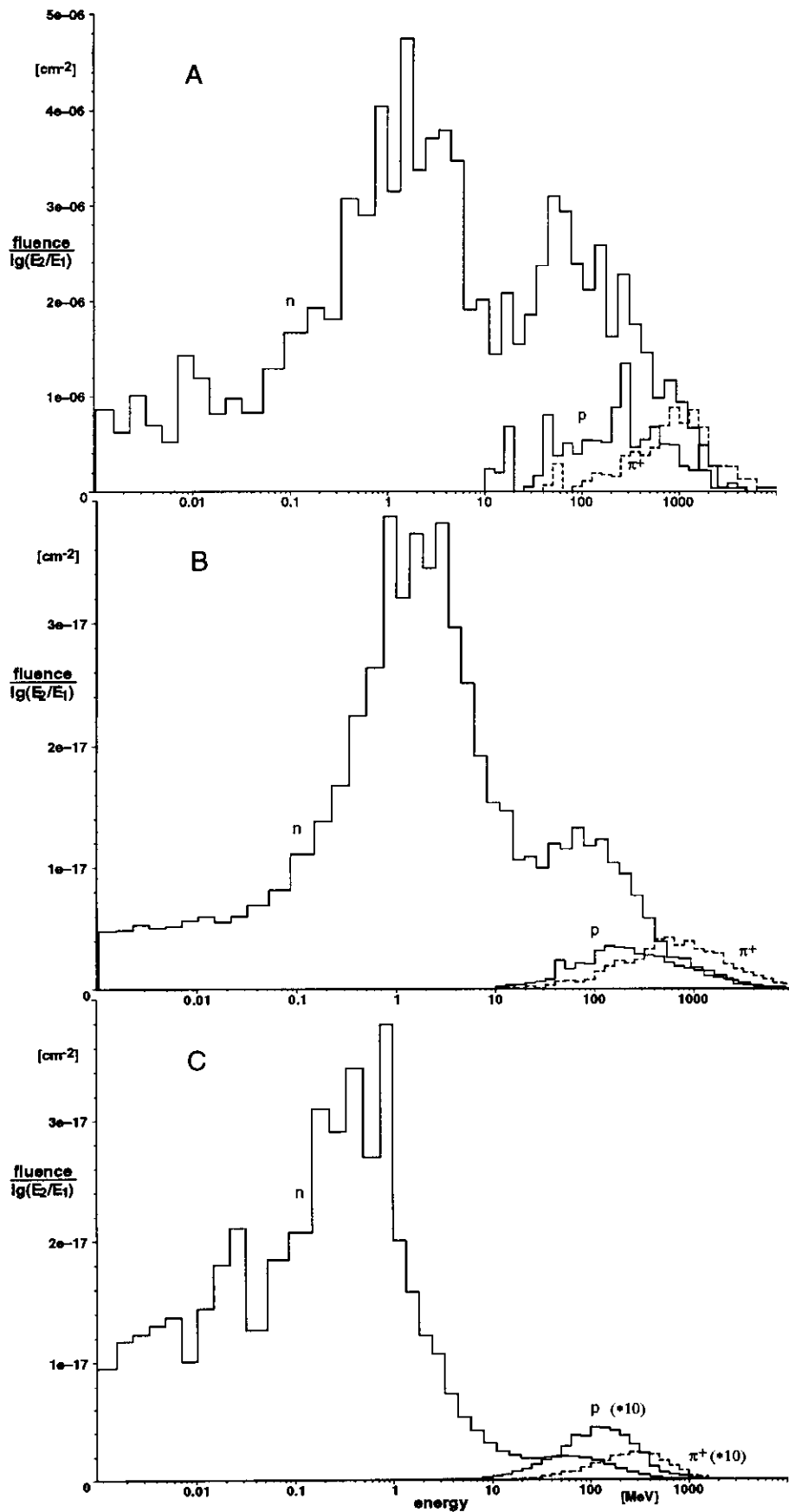


Figure 6: Calculated hadron fluences per logarithmic energy interval per primary proton: A) from the collimator, geometry Ia. B) from rest gas, geometry Ib. C) from rest gas, geometry II.

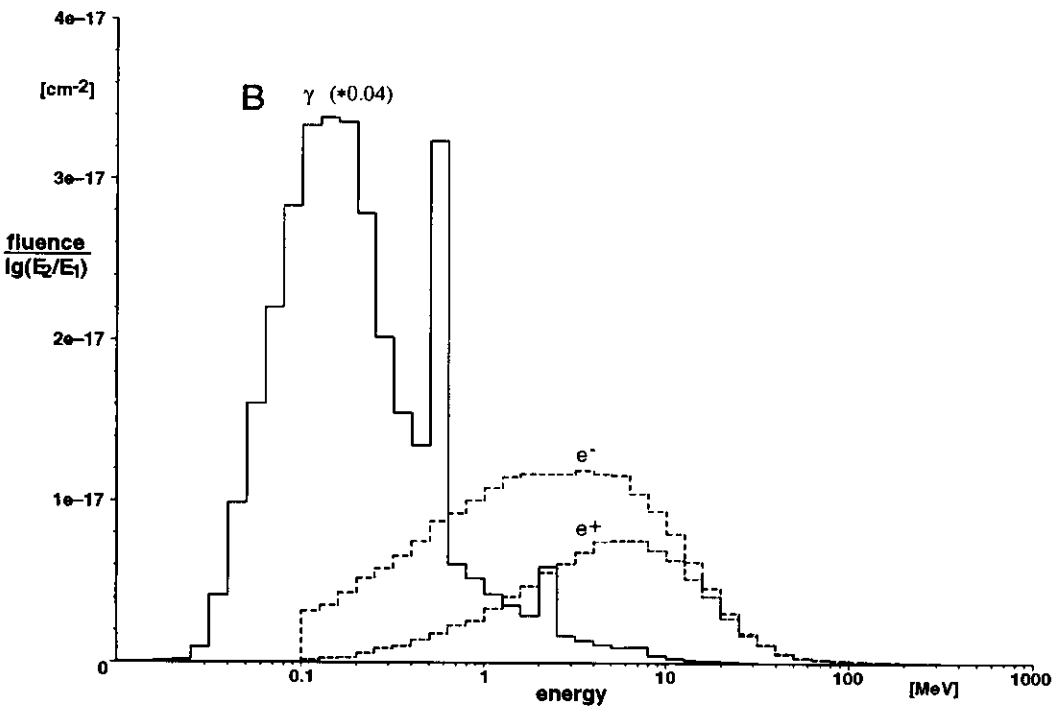
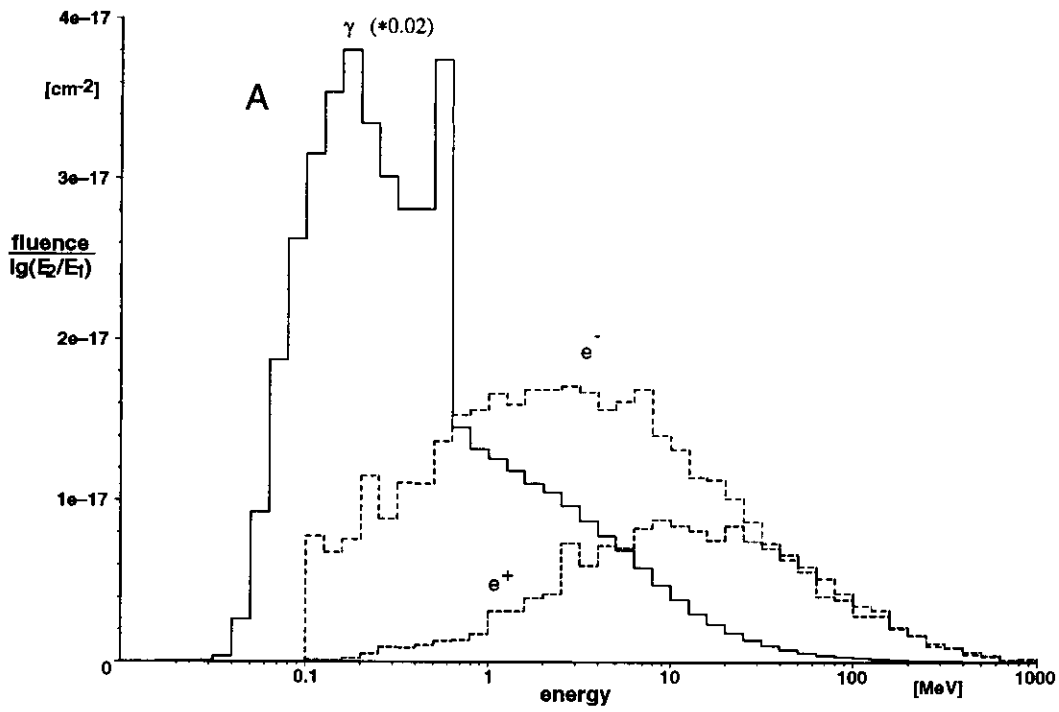


Figure 7: Calculated fluences per logarithmic energy interval per primary proton: A) Geometry I, B) Geometry II.